The EMBO Journal vol.11 no.12 pp.4653-4663, 1992

Transcription of human c-*myc* in permeabilized nuclei is associated with formation of Z-DNA in three discrete regions of the gene

Burghardt Wittig[1], Stefan Wölfl[1,2], Tomislav Dorbic[1], Wolfgang Vahrson[1] and Alexander Rich[2]

Institut für Molekularbiologie und Biochemie, Bereich Molekularbiologie und Bioinformatik, Freie Universität Berlin, Arnimallee 22, D-1000 Berlin, Germany, and [2]Department of Biology, Massachusetts Institute of Technology, Cambridge, MA 02139, USA

Communicated by A.Rich

When human U937 cells are placed in agarose microbeads and treated with a detergent, the cytoplasmic membrane is lysed and the nuclear membrane is permeabilized. However, the nuclei remain intact and maintain both replication and transcription. Biotin labeled monoclonal antibodies against Z-DNA have been diffused into this system and used to measure the amount of Z-DNA present in the nuclei. It has previously been shown that the amount of Z-DNA present decreases due to relaxation by topoisomerase I and increases as the level of transcription increases. Here we measure the formation of Z-DNA in the c-*myc* gene by crosslinking the antibodies to DNA using laser radiation at 266 nm for 10 ns. The crosslinked DNA is isolated by restriction digestion, separation of antibody labeled fractions through the biotin residue, and subsequent proteolysis to remove the crosslinked antibody. Three *Alu*I restriction fragments of the c-*myc* gene are shown to form Z-DNA when the cell is transcribing c-*myc*. The Z-DNA forming segments are near the promoter regions of the gene. However, when U937 cells start to differentiate and transcription of the c-*myc* gene is down-regulated, the Z-DNA content goes to undetectable levels within 30-60 min.

Key words: c-*myc*/DNA conformation/transcription/Z-DNA

Introduction

DNA in the chromatin of organisms is in a dynamic state. A number of physiological processes are associated with changes in the torsional strain of the molecule which in turn facilitates conformational changes in DNA. One of the most dramatic of these changes is the conversion from the right-handed B-DNA to the higher energy left-handed Z-DNA form. The conversion of DNA from the B to the Z form has been studied in many systems (Rich *et al.*, 1984; Jovin *et al.*, 1987; Hill, 1991). However, only recently has it been possible to demonstrate the formation of Z-DNA *in vivo* or in systems that are very close to that found in the living cell (Rahmouni and Wells, 1989; Wittig *et al.*, 1989; Jimenez-Ruiz *et al.*, 1991). One of the systems that has proven of great value is the preparation of metabolically active nuclei developed through the work of Jackson and Cook (Jackson and Cook, 1985; Jackson *et al.*, 1988). They encapsulated mammalian cells in agarose microbeads. Upon addition of Triton X, the cytoplasmic membrane is lysed and the nuclear envelope permeabilized. In the protective environment of the agarose microbead, these nuclei retain significant normal metabolic features. They replicate DNA at a rate 85% of that seen in the intact cell and they are active in transcription (Jackson *et al.*, 1988). We have used these nuclei previously to demonstrate the formation of Z-DNA (Wittig *et al.*, 1989). This was accomplished by using a monoclonal antibody that is specific for the zigzag backbone of Z-DNA and has a biotin molecule attached to it. The biotin labeled monoclonal antibody is allowed to diffuse inside the nucleus and the amount of the antibody can be measured by the subsequent addition of radioactively labeled streptavidin. Experiments using this antibody as well as a control antibody directed against a non-histone chromosomal protein, HMG-17 (Dorbic and Wittig, 1987), demonstrated that the nucleus is labeled throughout its volume. On varying the amount of antibody equilibrated with the encapsulated nuclei, a plateau region was found in which the Z-DNA specific antibody concentration could be changed 100-fold and yet the amount of binding in the nucleus was unchanged. The height of this plateau region was related to the torsional strain of the DNA in the nucleus. Loss of torsional strain led to loss of antibody binding while increasing the torsional strain through inhibiting topoisomerase I led to increased antibody binding (Wittig *et al.*, 1990).

These first experiments demonstrated that the continued activity of topoisomerase I led to a continued decrease in the amount of antibody bound to Z-DNA. Subsequent experiments demonstrated that transcription was the major process that generated Z-DNA, while replication had a much smaller effect in increasing the level of Z-DNA in the nucleus (Wittig *et al.*, 1991). We surmised that this might be associated with the phenomenon described by Liu and Wang in which the movement of RNA polymerase along a DNA strand is associated with the generation of positive supercoils downstream and negative supercoils in the upstream region (Liu and Wang, 1987). The negative supercoiling generated by transcription would act to stabilize the Z-DNA conformation. Thus, the DNA in chromatin is in a dynamic state in which transcription generates Z-DNA and topoisomerase I relaxation results in its decrease.

These experiments were global in nature in that they did not address the activities of individual genes but rather measured the total effect of either transcription or topoisomerase I relaxation on Z-DNA content. Here we describe the formation of Z-DNA in a specific gene, the c-*myc* proto-oncogene which is transcribed at a high rate in cells that are rapidly dividing (Cole, 1986; Piechaczyk *et al.*, 1987). This measurement was carried out through the use of a high intensity laser at 266 nm which selectively produces crosslinks between proteins and DNA but does not crosslink proteins (Budowsky and Abdurashidova, 1989; Stefanovsky *et al.*, 1989; Kovalsky *et al.*, 1990). Exposing metabolically

active nuclei to the laser for 10 ns crosslinks DNA to antibody. The efficiency is great enough to permit isolation of those segments of DNA to which antibody is bound. The specific loci where Z-DNA formation occurs in the c-*myc* gene associated with transcription were determined by restriction analysis. Furthermore, we show that the formation of Z-DNA is turned off rather rapidly after the cell is given the stimulus to differentiate in which the c-*myc* transcription is also down-regulated.

Results

Human myelomonocytic U937 cells (Sundström and Nilsson, 1976) transcribe the c-*myc* proto-oncogene at a high rate (Einat *et al.*, 1985). The c-*myc* mRNA is known to have a rapid turnover with a half life of 10–15 min (Piechaczyk *et al.*, 1985). C-*myc* may assist in pushing the cells from the G_0 to the G_1 phase (Einat *et al.*, 1985). Treatment of U937 cells with a phorbol ester (PMA) together with a vitamin D derivative effectively induces differentiation down the monocyte/macrophage pathway (Gidlund *et al.*, 1981). Cell proliferation then slows down and synthesis of c-*myc* ceases (Pauza *et al.*, 1988; Karmali *et al.*, 1989). This system represents an ideal one in which the presence of Z-DNA can be measured and correlated with the transcription of the gene.

The technical discovery that made this measurement possible was the observation that exposure of metabolically active permeabilized nuclei in agarose microbeads to high intensity laser light at 266 nm for 10 ns gave a reasonably high efficiency of crosslinking of antibody to DNA. Using restriction endonucleases, we extract fragments of DNA from the nucleus and the subfraction containing antibodies bound to DNA can be isolated. The general protocol for these preparations is outlined in Figure 1. Incorporation of cells growing in tissue culture into agarose microbeads, subsequent treatment with Triton X to produce permeabilized nuclei and the time for equilibrating biotin labeled monoclonal antibodies in the nuclei have been described previously (Jackson and Cook, 1985; Wittig *et al.*, 1989). It takes ~2 h for the monoclonal antibodies to diffuse into the nuclei and reach an equilibrium concentration.

An important consideration in binding the monoclonal antibody to the nucleus is the concentration of antibody. It has been shown previously that there exists a plateau concentration region, i.e. a region in which the antibody concentration can be changed up to 100-fold with no increase in antibody binding. At much higher concentrations of antibody increased antibody binding is observed due to the 'induction' of Z-DNA by the antibody itself (Wittig *et al.*, 1989). In the experiments described here, a concentration of antibody was used in the middle of the plateau region so that it would provide a measure of the level of intrinsic Z-DNA in the nucleus. Subsequent to equilibration of the antibody in the nucleus, the microbeads were exposed for 10 ns to a high intensity neodynium YAG laser. This was followed by an incubation with 2 M sodium chloride which facilitated the release of many proteins from the nucleus as well as of unbound antibodies. Restriction endonuclease was then diffused into the system to cleave the genomic DNA. For these experiments, we chose the enzyme *Alu*I which cleaves at the sequence AGCT, in order to get a sufficiently fine resolution of genome fragments using the known *Alu*I restriction sites in the c-*myc* gene.

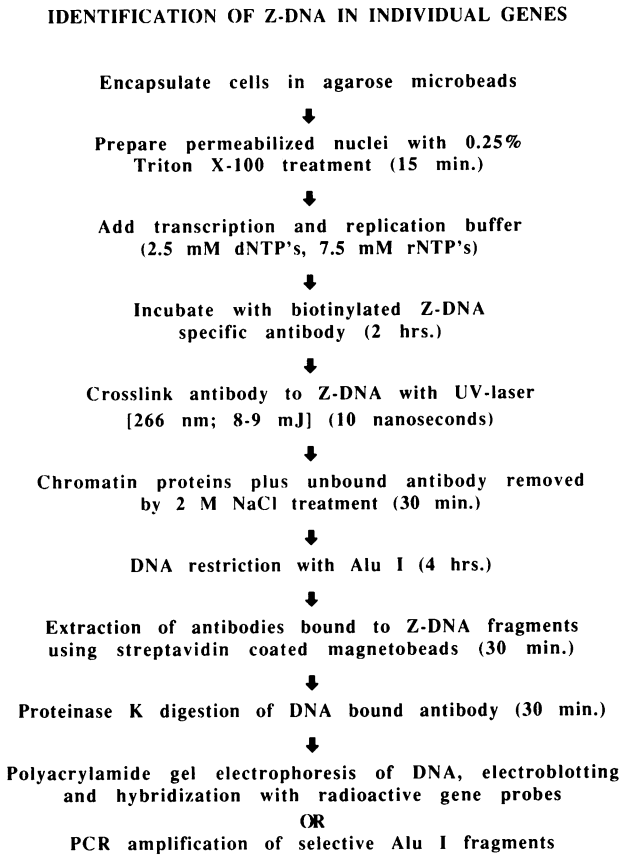

Fig. 1. An outline of the protocol used in identifying Z-DNA in individual genes. The time periods for various steps are indicated in parentheses.

Manipulations with the agarose encapsulated permeabilized nuclei are carried out quite easily as the physical integrity of the nucleus is protected by the microbead environment. The microbead solution can be centrifuged at low *g* and formed into a pellet. The supernatant can be withdrawn and then the agarose microbeads resuspended. During frequent washing of this type the DNA remains unbroken prior to restriction enzyme digestion. Following the lengthy incubation with *Alu*I, DNA fragments emerge from the nuclei. Most of them are free fragments but a small proportion are crosslinked to the monoclonal antibody. The latter fraction can be rapidly purified through the use of streptavidin coated magnetobeads (Dynabeads®). These beads are incubated with the supernatant for a short time period and then a magnet allows these magnetobeads to be separated from the remaining supernatant. The DNA restriction fragments which emerge following digestion are thus separated into two fractions, an unbound fraction which remains in solution, and a bound fraction attached to the magnetobeads.

The bound DNA is released from the magnetobeads by incubation with proteinase K. This digests the antibody bridge between the DNA and the magnetobeads. The digestion yields a mixture of DNA restriction fragments that initially had the antibody attached to them. However, they are now clear of the antibody with the exception of amino acid remnants that may remain at the crosslinking site. These DNA restriction fragments can now be used to carry out either a hybridization to detect which ones are present or a polymerase chain reaction (PCR) which enhances the

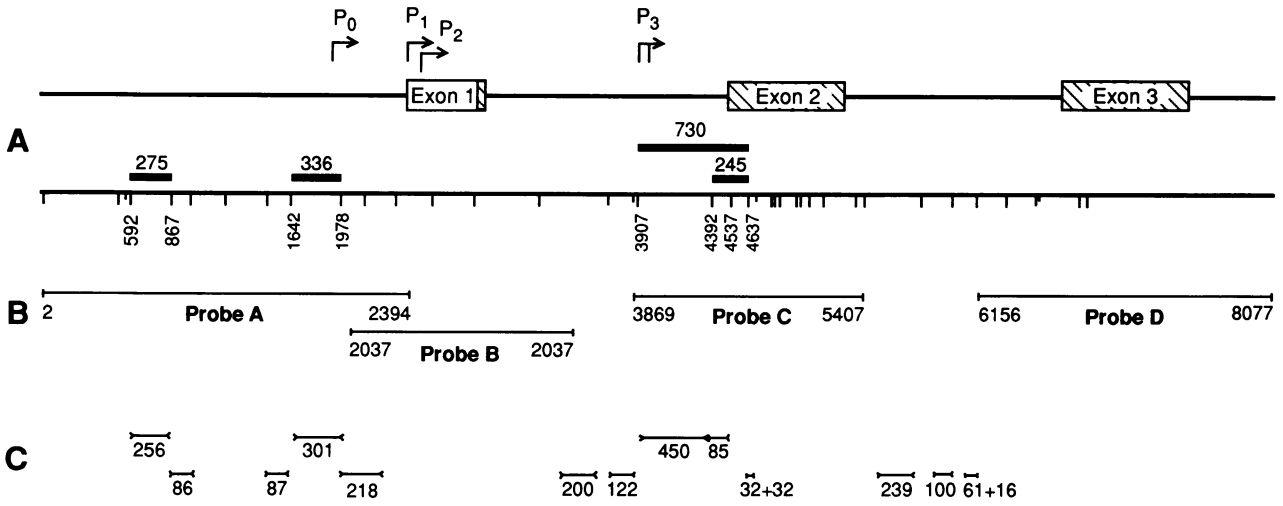

Fig. 2. A diagram illustrating the c-*myc* gene and various points of interest. The c-*myc* gene is shown at the top together with its three exons and four promoters, P0, P1, P2 and P3. The crosshatched areas on exons 1, 2 and 3 represent the structural gene for the 67 kDa protein. (**A**) The 8 kb *Hin*dIII−*Eco*RI segment is shown together with vertical lines which indicate the site of *Alu*I restriction enzyme cleavage. The numbers indicate the nucleotide positions at the ends of the three hybridizing *Alu*I fragments, which we call Z1, Z2 and Z3 left to right. The numbers above them are the lengths of the fragments in nucleotides. (**B**) The position of the four hybridization probes is shown together with the nucleotide numbers of the first and last nucleotides. RNA hybridization probes A−D were generated with T7 or Sp6 RNA polymerase from plasmids containing the indicated c-*myc* gene fragments. (**C**) The positions of various *Alu*I fragments that were used for PCR amplifications are indicated. The number refers to the nucleotide length of the PCR product. These PCR fragments include segments that form Z-DNA, Z1, Z2 and Z3 as well as a number of additional fragments which were used to cover gaps between hybridization probes, or fragments that flank the Z-forming sections. In some cases, PCR products longer than *Alu*I fragments are generated using PCR primers with non-specific tails. These PCR products could then be detected by gel electrophoresis.

sensitivity for detecting small amounts of fragments present in the solution.

This DNA preparation contains all of the DNA fragments that had antibody attached, i.e. they come from many different genes. In the experiments carried out here, we assay for a subset of these DNA fragments related to the c-*myc* gene. This preparation can also be used to search for Z-DNA containing fragments from other genes as well.

Hybridization studies

Figure 2 contains an outline of the c-*myc* gene. The *Hin*dIII−*Eco*RI fragment shown encompasses the three exons found in the gene as well as a large segment of the region upstream of the first exon. The gene is known to have four different promoters as indicated in the diagram. The 67 kDa protein, one of the two major gene products, is represented by crosshatched areas. Below the gene in Figure 2, the *Alu*I restriction fragments are shown by a series of vertical lines. The search for restriction fragments in the DNA bound to the magnetobeads was carried out by hybridization experiments using four different RNA probes, A−D, as indicated in the diagram.

The hybridization experiments are shown in Figure 3. Figure 3a shows the results for probe A. The first lane contains 5 μg of genomic DNA that had been digested with the *Alu*I restriction enzyme. The second lane has 0.5 μg. The numbers at the left represent the lengths in base pairs (bp) of the known *Alu*I fragments of the gene capable of hybridizing with probe A. The heavy loading in the column at the left yields two extra hybridization bands between 336 and 528 bp. However, those are not major components of the restriction digestion as they are no longer seen when 0.5 μg is applied to the column. Hybridization was carried out with DNA that was unbound (lane 3), i.e. remained in solution once the magnetobeads extracted the DNA. The third lane shows the hybridization produced by using 1/20 of the volume of the unbound fraction (0.05 unbound). The unbound fraction is seen to contain all of the restriction fragments found in the digestion of the genomic DNA. The fourth lane has one quarter of the bound DNA (0.25 bound); however, it was not exposed to the laser. The fifth lane on the right has the same 0.25 of the bound DNA, but it was exposed to the laser. This lane shows two hybridization bands with lengths of 336 and 275 nucleotides. The remaining eight bands of the restriction digestion do not appear in the hybridization. Figure 2A indicates the position of the restriction fragments of lengths 275 and 336.

Figure 3b shows the results with probe B from Figure 2. The same five columns are shown as in Figure 3a. Six genomic fragment bands are seen in the lane with 0.5 μg genomic DNA. The column with 0.05 unbound fraction shows all of the genomic fragments found in the lane containing 0.5 μg of genomic DNA plus one additional band labeled length (880). That length is equal to the sum of the two adjacent fragments, 454 and 426 bp, and probably arises from incomplete cleavage of the DNA. Incomplete *Alu*I digestion may also account for the fainter bands found in the lane containing 5 μg of DNA. The length of the fragments found in Figure 3 were measured by comparison with a standard *Hae*III restriction digest of φX174 DNA. The positions of the X174 marker fragments are shown in Figure 3c.

The hybridization results from probe C (Figure 2) are shown in Figure 3c. The lane containing 0.5 μg of DNA shows nine hybridization bands from the *Alu*I digest. The lane containing 5 μg of DNA contains in addition several weaker bands which undoubtedly arise from incomplete *Alu*I digestion. In the lane containing 0.05 μg of the unbound fraction, all nine restriction fragments appear. In addition, there is another more slowly moving band labeled (730).

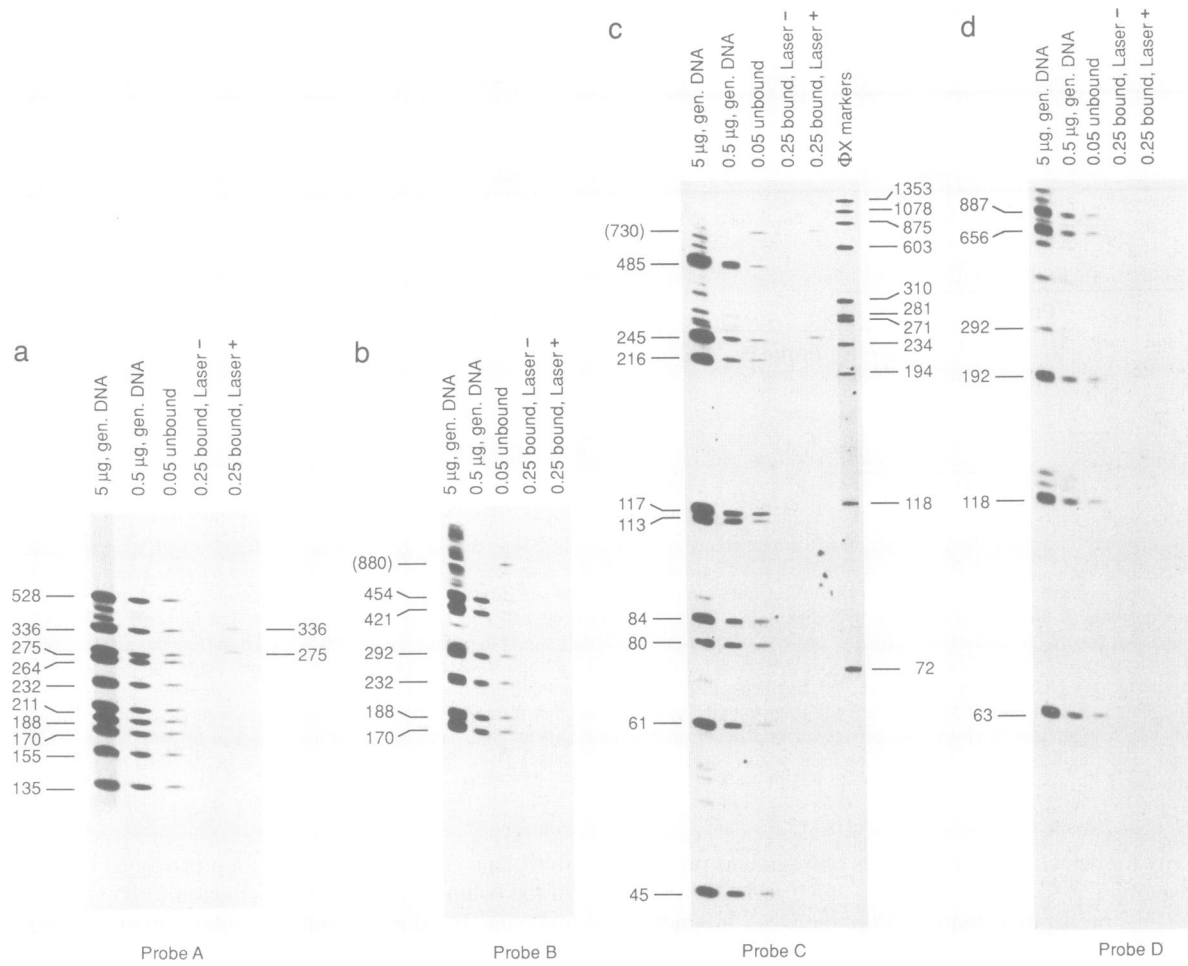

Fig. 3. Hybridization of *Alu*I fragments that were bound to streptavadin coated magnetobeads and then released with proteinase K digestion. These fragments were electrophoresed in an 8% polyacrylamide gel and then transferred to a nylon membrane for hybridization. The first two lanes in each panel show a restriction digest of genomic DNA with a loading of 5 and 0.5 µg respectively. The lengths of the major *Alu*I fragments are indicated to the left. Lane 3 contains 5% of the fraction of DNA not bound to the magnetobeads. Lanes 4 and 5 contain 25% of the DNA that had been bound to the magnetobeads and then freed by proteinase digestion. The material in lane 4 did not have laser irradiation, while lane 5 did. (**a**) The results are shown for probe A. Ten major genomic bands are produced by *Alu*I digestion and two of the bands (336 and 275 nucleotides) are found in the bound fraction that had been exposed to the laser. (**b**) Hybridization is carried out with probe B. It can be seen that six major bands are found in the genomic DNA. The unbound fraction in lane 3 showed a band of 880 nucleotides indicated in parentheses. It represents an incomplete *Alu*I cleavage between the two adjacent bands containing 454 and 426 nucleotides. It can be seen that those bands are much weaker on that lane. Size markers (not shown) were used. No bands are positive in the laser irradiated sample. (**c**) The hybridization with probe C yielded nine major genomic DNA bands. Lane 6 has a restriction digest of X DNA used as size markers. The unbound fraction in lane 3 has a band containing (730) nucleotides which arises from partial *Alu*I digestion of the two adjacent bands containing 485 nucleotides and 245 nucleotides. Without laser irradiation, lane 4 has no bands; however, lane 5 with laser irradiation shows positive bands at 245 nucleotides as well as one with (730) nucleotides that arises from incomplete *Alu*I digestion. It should be noted that the band at 245 nucleotides in lane 5 migrates slightly more slowly than the band that arises from the unbound DNA in lane 3. This may be due to remnants of protein following proteinase K digestion. (**d**) In hybridization with probe D, five major bands can be found from the genomic DNA and none of these bands is visible in lane 5.

This band arises from incomplete digestion of the *Alu*I fragments containing 484 and 245 bp which are found adjacent to each other on the restriction map. As before, the lane containing one quarter of the bound DNA from non-irradiated nuclei shows no hybridization fragments. However, the lane containing bound DNA from nuclei that were irradiated with the laser shows a band at 245 bp and the band shown at (730) which arises from incomplete *Alu*I digestion. The remaining eight bands of the *Alu*I restriction site are not labeled by this hybridization probe. The position of both the 245 band as well as the (730) band is shown on the *Alu*I restriction digestion map in Figure 2.

The hybridization results with probe D are shown in Figure 3d. Five intense *Alu*I restriction sites are shown and none of them forms a hybridization complex with bound DNA from laser irradiated nuclei. From the four hybridization probes A−D, 30 *Alu*I restriction fragments were identified and three unique fragments (not counting the band due to incomplete cleavage) hybridized in fragments that were bound to the magnetobeads following laser irradiation. These experiments were repeated twice and the results were identical.

PCR experiments

The polymerase chain reaction (PCR) has been widely used as a sensitive method of detecting DNA that may be found in small amounts (Saiki *et al.*, 1988). We have used the PCR reaction in this study for two reasons. First, it allows us to

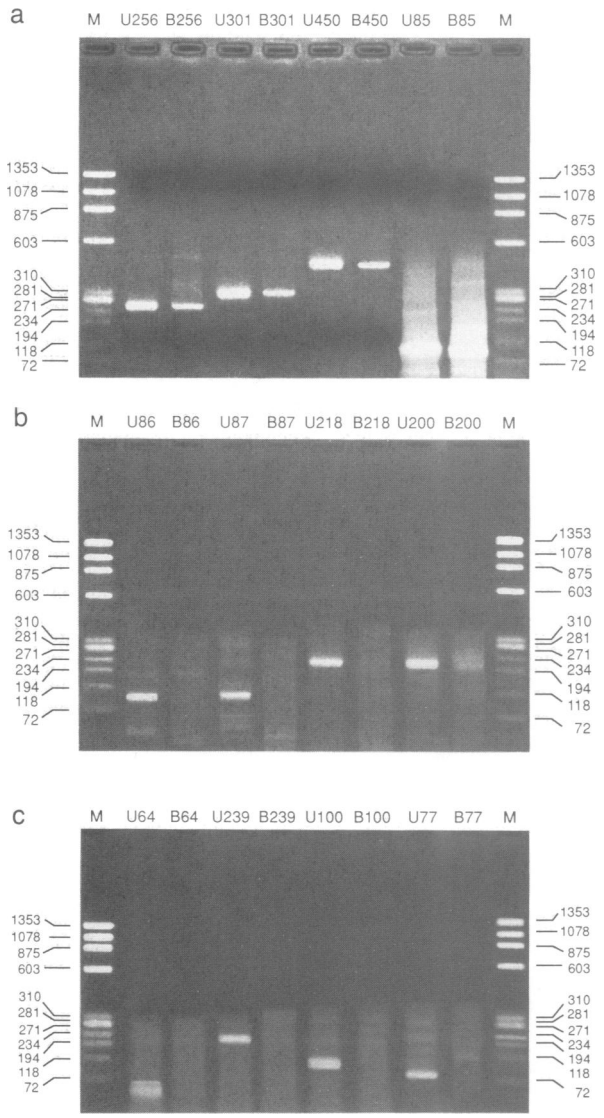

Fig. 4. DNA produced by PCR reactions is analyzed by electrophoresis in 2% agarose gels followed by staining with ethidium bromide. (**a**) The columns to the right and the left represent ϕX length markers (M) with their sizes indicated. Four different pairs of DNA were subjected to PCR amplification. The pairs were obtained from the unbound (U) and the bound (B) DNA pools. The bound DNA pool adhered to the streptavadin coated magnetobeads and was released with proteinase K digestion. The lanes with unbound fractions contained 2% of the material while the bound fractions contained 10% of the DNA. The fraction labeled 256 was derived from the Z1 *Alu*I fragment containing 275 nucleotides. Fraction 301 was obtained from the Z2 *Alu*I fragment 336 bp long. Fractions 450 bp long were obtained from the incompletely cleaved *Alu*I fragment connected to Z3, 730 nucleotides long. Fractions 85 nucleotides long came from the 245 nucleotide Z3 fragment. All of the bound fragments produced a PCR signal which migrated next to the stronger signal produced by the unbound material. (**b**) PCR amplification of *Alu*I fragments flanking the Z-DNA forming regions. Four different bound and unbound *Alu*I fragments are shown here. The positions of fragments 86, 87, 218 and 200 are shown in Figure 2. They are found on the 3′ and 5′ sides of the fragments Z1−Z3. The unbound fragments give strong ethidium bromide staining bands while the bound fragments produce no signal. (**c**) Fragment 64 is on the 5′ side of Z3 while fragments 239, 100 and 77 are found in the gap regions between probes C and D in Figure 2. The flanking fragment as well as the three fragments found in the gap produce no PCR staining signal in the bound fragments while the unbound fragments show a strong signal.

use the high sensitivity to explore whether fragments that are negative in hybridization are actually negative in the PCR reaction as well. In addition, we can use the PCR reaction to cover gaps between the probes that were used for hybridization as shown in Figure 2. Figure 2C shows a number of *Alu*I fragments for which primers were developed and PCR reactions were carried out. These include fragments that were either positive or negative in the hybridization reaction plus fragments found in regions that were not covered by the hybridization probes. The fragments are referred to by the number of base pairs predicted for the respective PCR synthesis product.

PCR primers 15−20 nucleotides long which had the necessary specificity and the requisite hybrid stability to produce an effective PCR reaction were selected using a computer search program (MacMolly® Tetra). Figure 4a shows the results for four different pairs of primers selected from those *Alu*I bands that gave a positive result in hybridization. Primers were used for the *Alu*I fragments containing 256 and 301 nucleotides which gave positive hybridization bands from probe A as shown in Figure 2. PCR primers were also used for products containing 85 and 450 bp; the former came from the 245 bp long *Alu*I restriction fragment while the latter came from the additional segment which was bound to that *Alu*I fragment due to incomplete *Alu*I cleavage. The results in Figure 4a are shown together with an *Hae*III restriction ladder of known lengths from ϕX174 DNA. In carrying out the PCR reaction, an attempt was made to put roughly equivalent amounts of template DNA from either the unbound or the bound fragments in the starting reaction mixture. It was found that the concentrations of DNA in both the unbound and the bound fragments were such that 1 μl of the unbound fraction contained an amount of DNA roughly equal to that found in 5 μl of the bound fragments. Additionally, for each of the four pairs of lanes shown in Figure 4a, the volume of DNA actually loaded for agarose gel electrophoresis was inversely proportional to the number of base pairs in the fragments. Thus, a greater amount of DNA was loaded of the 85 bp product than of the products of greater length.

Following staining with ethidium bromide, the gels were photographed using transilluminated UV light. PCR products were synthesized from all of the primers using template DNA from the bound fraction as well as from the unbound fraction (Figure 4a). The intensities of the band pairs are not identical, but this can be due to a number of things including variable efficiency of the priming process as well as errors in estimating the amount of DNA to be added as template initially. Figure 4b and c contain the results of PCR reactions using primers from regions that were negative in the hybridization reaction as well as from regions that were not covered by the hybridization probes. The position of these PCR fragments is shown in Figure 2. As in Figure 4a, roughly equal amounts of template DNA were added from both the unbound and the bound fractions. None of these primer pairs produced a band after PCR amplification of the bound fraction. Since the expected products were all produced from template DNA in the unbound fraction, experimental problems can be excluded. A number of weak, minor bands are found in Figure 4b and c which probably represent non-specific priming of other fragments in the reaction. These results reinforce the conclusions obtained

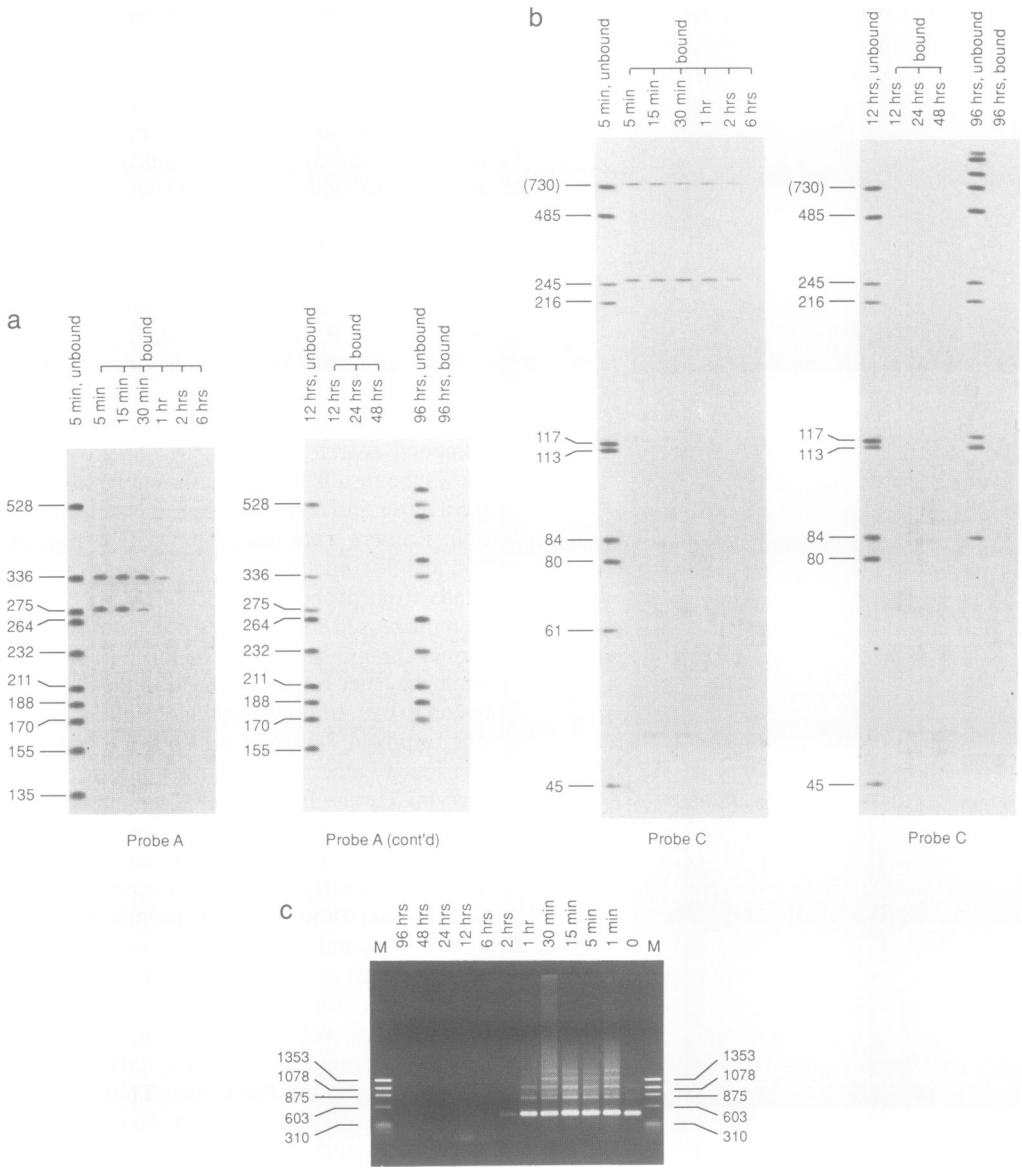

Fig. 5. The time course of Z-DNA formation following the exposure of U937 cells to differentiation agents. (**a**) Hybridization experiments are shown for probe A for varying time periods. The column on the left shows unbound DNA which was obtained 5 min after the onset of differentiation. The *Alu*I restriction fragments are identified by their length in a manner similar to that seen in Figure 3a. The remaining six lanes to the right represent DNA bound to the streptavidin coated microbeads after the cells had been exposed to the differentiation agents for the time periods indicated from 5 min to 6 h. The two positive hybridization bands at 336 and 275 nucleotides are seen up to 30 min. However, by 1 h, the 275 nucleotide band is no longer visible while the 336 nucleotide band is very faint and disappears in the following lane. The second gel shows the experiment continuing for longer time periods. The last two lanes show the DNA obtained from the unbound and bound fractions at 96 h. No bands are seen in the bound fraction at 96 h. However, there has been a change in the pattern of bands in the unbound fraction which is visible at 96 h. (**b**) Hybridization of DNA is shown for probe C as a function of time of exposure to differentiating agents. The column at the left shows the *Alu*I restriction digestion pattern from the unbound DNA fraction at 5 min. All the bands are present as seen in Figure 3c, including the fragment with length (730) due to partial digestion of one *Alu*I site. The six columns to the right represent DNA obtained from the bound fractions for time periods ranging from 5 min to 6 h. Fraction 245 as well as the partial digestion fragment (730) are both visible at 2 h and no longer at 6 h. These fractions both migrate somewhat more slowly than the fragments obtained from the unbound material. The second panel shows the results for longer time periods. The last two columns show the results for 96 h. No signal is found in the lane dealing with the bound fragments, but the unbound fragments have a pattern which is slightly different from that seen at 12 h. (**c**) The time course of differentiation and its effect on DNA in the bound fragments is illustrated using PCR amplification. Following PCR incubation the fragments were electrophoresed on 1% agarose and stained with ethidium bromide. Results are shown for the 450 bp PCR product obtained from the 730 bp Z3 *Alu*I fragment which arises from incomplete *Alu*I digestion. Following differentiation, the 450 bp fragment is seen strongly at 1 h, weakly at 2 h and is absent at 6 h, in agreement with the hybridization experiments (probe C).

from the hybridization reaction. Even using a more sensitive assay involving PCR amplification, no DNA fragments were obtained other than those which gave positive results in hybridization. Those reactions produced an amplified product while all of the others in Figure 4b and c were negative.

The effect of cell differentiation on Z-DNA-containing fragments

As mentioned above, the c-*myc* proto-oncogene effectively stops transcription in U937 monocytic leukemia cells on addition of a phorbol ester (PMA) as well as a vitamin D

derivative (Pauza *et al.*, 1988). The question we address in this section is what is the effect of this differentiation process on the presence of Z-DNA-containing fragments in the c-*myc* gene? Our previous global studies indicated that there was a direct correlation between transcriptional activity and Z-DNA formation (Wittig *et al.*, 1991). However, here we are able to ask whether for an individual gene, the effect of stopping transcription is reflected in a change in the amount of Z-DNA found in the gene.

The experiment was carried out by exposing intact cells to the phorbol ester and vitamin D derivative for varying time periods, following which the cells were encapsulaed in agarose microbeads. During the encapsulation process the externally added phorbol ester and vitamin D derivative are washed away and the experimental protocol outlined in Figure 1 is carried out. It should be pointed out that differentiation towards a monocyte/macrophage involves adhesion (Larsson *et al.*, 1988), morphological changes (Gidlund *et al.*, 1981) and the onset of phagocytosis (Dodd *et al.*, 1983) as well as changes in cell surface markers (Karmali *et al.*, 1989) that can be seen only after 12 h exposure to the differentiation agents. By 48 h after exposure to these agents, >90% of the cells in a tissue culture plate can be seen to have carried out the morphological transition to a monocyte.

Figure 5a and b shows the results of hybridization experiments carried out with probe A. Figure 5a (left) has in the left-hand lane an *Alu*I digestion of 0.05 μg of the DNA from the unbound fragments. A time course is shown in Figure 5a (left) ranging from 5 min to 6 h following exposure to the differentiation agents. Figure 5a (right) shows the results for 12 h up to 96 h. After 5 min exposure hybridization shows that the 336 and the 275 bp fragments are still attached to the magnetobeads in the bound fragment. The 336 bp band persists until 1 h and at 2 h the band has disappeared. The 275 bp band is already weakened considerably at 30 min and has disappeared by 1 h. Thus, these two bands disappear relatively quickly after exposure to the differentiation factors and well before cell adhesion or other morphological changes have taken place in the cell. The decay of c-*myc* transcription has been studied extensively following the addition of these differentiation factors (Pauza *et al.*, 1988; Karmali *et al.*, 1989). Figure 5a(right) shows that the bound fragments do not produce any hybridization band covering the period 12−96 h. It is interesting, however, that the unbound DNA fraction obtained from the 12 and the 96 h samples has a pattern of hybridization which is different from that found after 5 min exposure. These changes are probably associated with blocking certain *Alu*I sites in the nucleus so they are no longer susceptible to *Alu*I digestion.

The results of differentiation agents on probe C is shown in Figure 5b. In the absence of differentiation agents, bands at 245 and (730) were seen in the hybridization experiments. The latter band was attributed to incomplete *Alu*I digestion. After 5 min exposure of differentiation agents, bands are found at 245 and (730) nucleotides. The hybridization band at 245 nucleotides seems to be migrating at a slightly slower rate in this experiment, possibly due to variation in the proteinase K digestion. The bands at 245 and (730) are seen at 1 h, seen as weak bands at 2 h but are no longer seen at 6 h. The fact that both of these bands disappear after the same time exposure to the differentiation agent is consistent with the origin of the (730) band arising from an incomplete *Alu*I digestion. As noted in the results in Figure 5a with probe A, the *Alu*I bands which arise from the unbound fraction after 12 and 96 h of exposure to differentiation agents differ somewhat from that found after 5 min exposure. This probably also arises from changes in chromatin structure associated with differentiation.

In summary, the results of the hybridization experiments show that the Z-DNA forming segments disappear within 1−3 h following exposure to the differentiation agents.

The time course of the disappearance of the Z-DNA forming bands was also studied using the more sensitive method of PCR amplification. Figure 5c shows an example of the results of PCR amplification of bound DNA fragments which have been obtained from cells exposed to the differentiation factors for the varying time periods indicated, from 5 min to 96 h. The first and last lanes of this figure contain the *Hae*III restriction digest of φX174 DNA as markers. The PCR reaction was carried out using the same primers as in Figure 4a in lanes U450 and B450. Figure 5c shows that the 450 bp PCR product is present for 1 h but then disappears by 2 h. As mentioned above, the 450 nucleotide fragment arises because of an incomplete *Alu*I digestion (see Figure 2). The lengths of these PCR products are determined by the selection of primers that were used in the reaction. The background of fainter, slower migrating bands is probably due to false priming events becoming visible at the high amplification used. These results are qualitatively similar to the results obtained from the hybridization experiment, even though we are using a much more sensitive method to analyze for the presence of small numbers of DNA fragments.

These experiments illustrate that the three Z-DNA forming segments of the c-*myc* gene stop forming Z-DNA within a relatively short time period after they are exposed to differentiation agents as demonstrated by two different methods of analysis.

The effect of camptothecin, a topoisomerase I inhibitor

It has been shown previously that preincubation of the permeabilized nuclei before adding the monoclonal antibody is associated with a fairly rapid decline in the amount of antibodies that will bind to the nucleus (Wittig *et al.*, 1989). This decay was largely blocked through the addition of camptothecin, and it was interpreted as indicating that the DNA relaxing activity of topoisomerase I continued steadily throughout the preincubation period. Here we carry out the same type of experiment but look at the markers that are present in the hybridization found with probes A and C. Figure 6a shows the results with probe A which, as shown previously, produces positive bands with restriction lengths of 336 and 275 bp. In the absence of camptothecin, the 336 bp fragment shows a weak band at 1 h but nothing at 2 h. However, after 2 h of exposure to camptothecin, the 336 bp fragment is still weakly positive at 2 h and is absent by 3 h. The 275 bp band is barely seen in the absence of camptothecin after 1 h preincubation. In the presence of camptothecin, however, it is clearly seen at 1 h but not at 2 h.

Figure 6b shows the results for the hybridization fragments of length 245 bp as well as the (730) bp fragment associated with incomplete *Alu*I digestion. In the absence of camptothecin, the 245 and the (730) fragments are seen

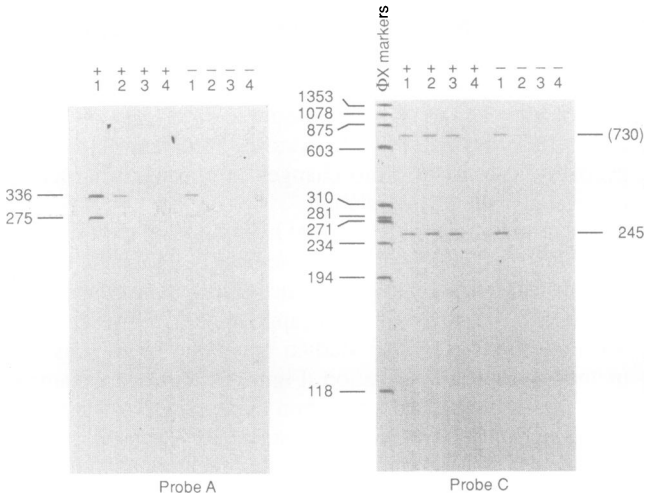

Fig. 6. Effect of camptothecin, a topoisomerase I inhibitor, on the time course of expression of Z-DNA following the addition of differentiation factors. (**a**) Results are shown for probe A1 through 4 h in the presence (+) or absence (−) of camptothecin. In the presence of camptothecin, hybridization produces a positive response after 2 h for fragment 336. However, it is only weakly positive after 1 h in the absence of camptothecin. Fragment 275 is positive after 1 h of camptothecin treatment, but is barely visible after 1 h in the absence of camptothecin. (**b**) Hybridization results are shown using probe C in the presence or absence of camptothecin. ϕX length markers are shown at the left. Both the *Alu*I fragment 245 and the longer fragment (730) produced by incomplete cleavage of the *Alu*I are seen. In the presence of camptothecin the hybridization signal remains positive up to 3 h, while in the absence of camptothecin it is positive for only 2 h with a very weak signal at that time.

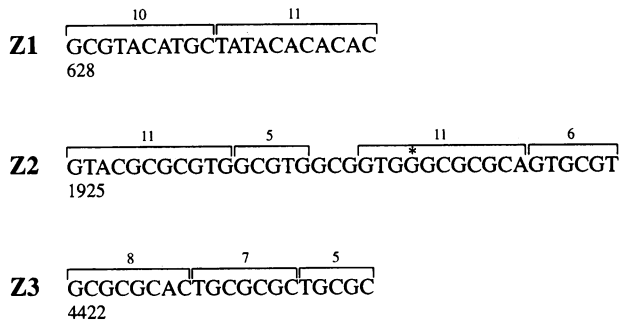

Fig. 7. The nucleotide sequence of the three segments of DNA with the highest potential for forming Z-DNA as determined by a computer scanning program. These three segments are found in the *Alu*I fragments Z1, Z2 and Z3. The number at the left indicates the nucleotide number of the sequence in the *Hin*dIII−*Eco*RI fragment containing the c-*myc* gene. The brackets indicate segments with alternations of purines and pyrimidines. A Z−Z junction is found where two brackets join. The numbers of nucleotides in the brackets are indicated. The asterisk indicates a nucleotide out of alternation.

weakly after 1 h incubation but virtually gone by 2 h. In the presence of camptothecin, they are both visible for 3 h but absent after 4 h. These experiments on the c-*myc* gene are thus in accordance with the global measurements made on Z-DNA binding associated with the inhibition of topoisomerase I (Wittig *et al.*, 1991). By inhibiting topoisomerase I, the Z-DNA forming fragments persist for a longer time period than in the absence of the inhibitor. Although topoisomerase I considerably lengthens the time period at which the c-*myc* fragments form Z-DNA, it does not lengthen it indefinitely. Either the inhibition of topoisomerase I by this amount of camptothecin is less than complete and the DNA continues to relax at a slow rate, or other processes are going on which result in loss of binding of Z-DNA specific antibodies.

PCR experiments were also carried out to measure the effect of camptothecin on the time period that the Z-DNA forming fragments of the *myc* gene persist following the addition of differentiation agents. These experiments (not shown) produced results that were virtually identical to those found in the hybridization experiments illustrated in Figure 6a and b.

Discussion

Following membrane lysis, the nuclei remain in their protective encapsulation, separate from each other, making it possible to use an isotonic buffer without nuclear clumping. In these nuclei, the DNA is intact and is replicated at 85% of the rate seen in the intact cell. The cells are active in continuing transcription, mostly elongation. However, the system is particularly robust and transcription goes on for many hours. These nuclei have been used for several studies and they appear to reflect most of the activities carried out in the intact cell (Jackson *et al.*, 1988).

We have identified Z-DNA formation in three *Alu*I fragments of the c-*myc* gene which we label Z1, Z2 and Z3. These fragments react with the monoclonal antibody against Z-DNA only when the gene is transcribed and not when it is inactive. Z-DNA is favored in alternating purine−pyrimidine sequences and alternating CG residues are more effective than alternating AT residues (Ellison *et al.*, 1986; Kagawa *et al.*, 1989). Several systems have been developed to determine the most probable Z-DNA forming sequences by calculating the energy of flipping GC or AT base pairs into the Z conformation as well as the energies found in the B−Z junctions (Ho *et al.*, 1986; Schroth *et al.*, 1992). This type of study was carried out with the c-*myc* gene. The three sequences with the highest probability of forming Z-DNA (Vahrson, 1991) are listed in Figure 7. They lie in the *Alu*I fragments Z1, Z2 and Z3. Experiments are currently being carried out to determine the precise location of the Z-forming sequences and will be reported elsewhere. The three most probable Z-forming sequences (Figure 7) have segments with 20 or more nucleotides which contain within them Z−Z junctions, where the phasing of alternations of purines and pyrimidines is interrupted (Johnston *et al.*, 1991). The energy of forming Z−Z junctions is considerably smaller than that found in B−Z junctions.

Antibodies are crosslinked to DNA by a 10 ns UV exposure. Proteins are removed by high salt extraction and the DNA is then restricted. Approximately 20% of the DNA comes out of the nuclei into the solution. Magnetobeads coated with streptavidin bind ~5% of the removed DNA while 95% is unbound. This does not allow us to estimate the efficiency of crosslinking because of numerous unknown variables. For example, is the sample that diffuses out of the nucleus representative of the 80% that remains inside? Nevertheless, the apparent efficiency of the procedure is surprisingly high, even though the UV crosslinking is carried out in a solution with significant concentrations of nucleoside triphosphates. This reduces the amount of radiant energy at the nucleus and accounts for the fact that very high energy (5−10 mJ) is required in order to produce the crosslinking.

Addition of the vitamin D derivative and phorbol ester to U937 cells results in a loss of Z-DNA formation within 1–2 h. The regulation of the c-*myc* gene is not well understood, however, it is known to be down-regulated rapidly during differentiation (reviewed by Lüscher and Eisenman, 1990; Spencer and Groudine, 1990). There are four different promoters in c-*myc*, all of which may be somewhat active even though P_1 and P_2 are the most significant (Eick *et al.*, 1990). Adding differentiation agents to U937 cells turns off c-*myc* synthesis fairly rapidly (Karmali *et al.*, 1989) which is consistent with the observed loss of Z-DNA. In measuring the cessation of Z-DNA formation, we have used two methods: hybridization to the *Alu*I fragments produced after varying time periods of exposure to differentiation agents as well as PCR amplification of these *Alu*I fragments. The Z-DNA segments formed in Z1 and Z2 turn off between 30 and 60 min while the Z3 formation is no longer detectable after 2 h. Since the transcription is largely elongation, it is possible that the time difference between Z3 compared with Z1 and Z2 may be due to the fact that it is further downstream and therefore would tend to register its signal at a later time. The results in the PCR amplification are similar to those observed with hybridization even though the former method is considerably more sensitive. It should be pointed out that 20 μl of solution is used for the hybridization experiment while only 1 μl is used as a template for the PCR reaction.

Schroth *et al.* (1992) have recently determined the occurrence and distribution of Z-DNA motifs in human genes. They analyzed 137 fully sequenced genes and using a computer program, they were able to calculate the potential these sequences had for flipping into Z-DNA based upon their sequence and the thermodynamic data concerning their stability. They found that >70% of the human genes in their collection had segments of DNA which would have a significant tendency to form Z-DNA under the stimulus of negative supercoiling. These segments are typically 12–15 nucleotides long and contain a high percentage of alternating cytosine and guanine residues. On average, each gene contained three such segments. However, the observed distribution is far from random. The Z-DNA motifs show a tendency to cluster near the 5′ end of the gene and in the promoter region. These are precisely the regions that would be most likely to form Z-DNA under the influence of negative supercoiling generated by RNA polymerase activity according to the twin domain model of Liu and Wang (1987). The distribution is the same as that found in the c-*myc* gene, with a high concentration of the sequences near transcription start sites and in the immediate upstream promoter area. The common occurrence of these sequences suggests that the phenomenon we are describing may in principle characterize a large majority of human genes.

The conformation of DNA appears to be in a dynamic state. During transcription of c-*myc*, Z-DNA formation occurs in three segments in the upstream region of the gene and fairly near the promoters. It may be the negative supercoiling generated in the wake of the RNA polymerase (Liu and Wang, 1987) that is responsible for Z-DNA formation during transcription; its decay when transcription stops is likely to be responsible for the loss of Z-DNA formation. As shown earlier, topoisomerases are continually acting upon Z-DNA and relaxing it into the B-DNA state (Wittig *et al.*, 1989, 1990).

Recent *in vitro* experiments demonstrate that a surprisingly high level of negative supercoiling is produced with transcription, and it diffuses away more slowly than would otherwise be expected (Dröge and Nordheim, 1991). It has been shown that it takes more energy to nucleate Z-DNA formation than to maintain it, probably due to a kinetic trapping. In the wake of a polymerase a high level of negative supercoiling is generated which, when found in a DNA sequence that has a relatively low threshold for flipping to the Z conformation, results in forming Z-DNA behind it and maintaining it for a considerable period as the polymerase continues.

RNA polymerase molecules are generally believed to be lined up on DNA awaiting the onset of transcription. Once transcription starts, these polymerase molecules start moving down the gene and transcribing it. In *Drosophila* embryo genes these RNA polymerase molecules can be seen in electron micrographs which show messenger RNA strands coming off and ribonucleoprotein particles attached to them (Beyer and Osheim, 1988). In these systems the polymerase molecules are fairly close together. However, we might ask what would happen when a polymerase passes by a DNA sequence with a high potential for forming Z-DNA. The negative supercoiling generated by the polymerase movement will stabilize the Z conformation in that segment. In *in vitro* experiments RNA polymerase is unable to transcribe through the Z-DNA conformation (Peck and Wang, 1985). This may result in delaying the transit of the following polymerase. Even though the following polymerase is generating positive supercoiling as it moves forward, the amount of positive supercoiling that it can produce may be limited through its being blocked by the Z-forming segment, while the negative supercoiling from the movement of the first polymerase molecule continues to generate the energy required to maintain the Z conformation. Thus, the second polymerase may have to wait until topoisomerase I diffuses into the system and relaxes it. Only when topoisomerase I relaxes the Z segment into B-DNA can the second polymerase pass by. This in turn will flip the Z-DNA forming segment behind it into the Z conformation and produce a transient halt in the movement of the third polymerase. The net effect of this repetitive process may be that the RNA polymerases which were close together as they initially moved down the gene at the start of transcription are separated by the transient formation of Z-DNA in the wake of each individual polymerase.

Unlike prokaryotic systems, eukaryotic transcripts undergo considerable processing, splicing occurs and introns are removed. Elongation and splicing appear to occur simultaneously (Eick, 1990). We speculate that polymerases that are close together on a DNA strand and have long RNA transcripts close to each other might produce a higher incidence of transplicing or erroneous splicing in which, for example, the upper splice site of one transcript is linked to a lower splice site of another transcript, producing an inappropriate or non-functional molecule. We suggest the possibility that Z-DNA formation associated with transcription may result in the separation of RNA polymerases which would have the effect of increasing the fidelity of RNA splicing so that a higher percentage of biologically active transcripts can be produced. It is possible to test such a model experimentally. For example, we could alter the nucleotide sequences in the Z-DNA forming regions so that they are no longer readily capable of absorbing the negative supercoiling energy to form Z-DNA. We might ask

whether this process leads to a larger percentage of aberrant splicing.

The Z-DNA forming sequence in Z1 is 1 kb upstream of promoter P_0. Could negative supercoiling generated near this promoter be responsible for flipping this sequence into the Z conformation? The answer is not entirely clear since negative supercoiling can also be generated by the removal of nucleosomes in chromatin associated with gene activation.

If we view Z-DNA forming segments as a sink for storing the energy of negative supercoiling associated with transcriptional activity, what do we conclude about those genes that appear to have a low probability of forming Z-DNA? Is it possible that those genes use the negative torsional strain to generate other conformational changes, such as cruciforms or triple helix formation in homopurine–homopyrimidine tracts? We can use the methodology described here as a way of addressing these questions.

The basic finding reported in this paper is that three segments in the upstream region of the c-*myc* gene convert to the Z-DNA form in a manner that is correlated with active transcription. The sequences which are presumed to have formed Z-DNA in the c-*myc* gene are not unusual, as similar sequences are found in a large number of human genes. We have made a suggestion above about a possible biological consequence of this conformational change associated with transcription, but other biological effects are also possible. Further investigation may make it possible to uncover the role of Z-DNA formation in biological systems. The methodology described in this paper can be used to analyze conformational changes in any single copy mammalian gene. It is likely that there will be numerous applications.

Materials and methods

Tissue culture, encapsulation of cells

U937 cells (ATCC #CRL 1593) were grown in RPMI 1640 medium (Gibco/BRL) with L-glutamine supplemented with $NaHCO_3$ (2 g/l), streptomycin (60 μg/ml)/penicillin (60 U/ml) (Gibco/BRL) and 10% (v/v) fetal bovine serum (Gibco/BRL). For differentiation, 10^8 cells were seeded onto tissue culture plates (245×245×20, Nunc) and both phorbol 12-myristate 13-acetate (PMA Sigma #P8139) and 1,25-dihydroxycholecalciferol (vitamin D3, kindly provided by Dr Milan Uskokovich, Hoffmann–LaRoche) were added to a final concentration of 10^{-8} mol/l each. At indicated times after addition of the differentiation agents, cells were encapsulated in agarose microbeads following the published procedure (Jackson and Cook, 1985; Wittig *et al.*, 1989). At differentiation times shorter than 1 h, adherent as well as suspended cells were encapsulated. For the longer time points only cells attached to the tissue culture plates were used.

Permeabilization of nuclei

Permeabilization was performed in 'new' buffer A [130 mM KCl, 1 mM $MgCl_2$, 1 mM Na_2ATP, 10 mM Na_2HPO_4, pH 7.4 (if necessary adjusted with KH_2PO_4) and 0.25% (v/v) Triton X-100] on ice for 20 min (Jackson *et al.*, 1988; Wittig *et al.*, 1991). Permeabilized nuclei were washed in buffer A without Triton X-100 by pelleting the agarose microbeads (2800 *g*, 15 min) and resuspending them in 40 ml of buffer A. The washing procedure was repeated three times. The agarose microbead pellet was then resuspended by adding a volume of buffer A roughly equal to the pellet volume. For each sample, 800 μl of encapsulated permeabilized nuclei corresponding to $\sim 4\times10^6$ nuclei were used in the following steps.

Binding of Z-DNA specific antibody

High concentrations of all four rNTPs [final concentration (f.c.) 7.5 mmol/l each] and all four dNTPs (f.c. 2.5 mmol/l each) were added. 2.8 μg biotinylated Z-DNA specific antibody Z 22 (Lafer *et al.*, 1981; Stollar, 1986) were added to each sample of $\sim 4\times10^6$ nuclei (Wittig *et al.*, 1991). The antibody was allowed to bind at room temperature (RT) for 2 h.

Crosslinking of antibody to Z-DNA with UV laser

The light source used was a Nd-YAG laser (Quanta Ray DCR-3). The fourth harmonic at 266 nm was used at an average pulse energy of 8 mJ. The pulse duration was 10 ns. The beam was focused on an area of 100 mm^2 and the energy was measured before the samples were irradiated. Samples were exposed to one pulse in a regular 1 ml UV grade quartz cuvette with 10 mm pathlength.

Isolation of Z-DNA fragments crosslinked to antibody

All samples were adjusted to a volume of 900 μl and 600 μl of 5 M NaCl were added (f.c. 2 mol/l). Samples were left on ice for 30 min and subsequently washed twice with 2 M NaCl to remove unbound proteins and RNA. The encapsulated nuclei were next equilibrated with three washes of *Alu*I buffer (10 mM $MgCl_2$, 50 mM Tris–HCl, pH 8.0). To the pelleted agarose beads, 250 μl of *Alu*I buffer were added and restriction digestion was performed with 100 U *Alu*I (BRL) in a rotating device at 37°C for at least 4 h. Agarose microbeads were pelleted and the supernatant of 300–350 μl recovered.

Streptavidin coated magnetobeads (30 μl) (Dynabeads®) were washed three times with 1×phosphate buffered saline (PBS). Supernatant (300–350 μl) from the *Alu*I restriction digest was added to the pelleted magnetobeads and suspended. Samples were left at room temperature (RT) for 30 min to allow binding. To prevent sedimentation, reaction vials were inverted and shaken every 5 min. Magnetobeads were separated with a magnet as described by the manufacturer. Supernatants from this step containing unbound DNA fragments, were collected and kept for further analysis. Magnetobeads were washed five times with 1×PBS. The magnetobead pellet was resuspended in 100 μl buffer [10 mM NaCl, 5 mM EDTA, 0.2% (w/v) SDS, 10 mM Tris–HCl, pH 8.0] and digested with proteinase K (f.c. 300 μg/ml) at RT. Reaction vials were inverted and shaken every 5 min to prevent sedimentation. After 1 h of incubation, RNase A was added (f.c. 25 μg/ml) and reaction continued for an additional 30 min. DNA fragments were separated by phenol/chloroform/isoamylalcohol extraction and precipitated with ethanol.

Supernatant from the magnetobead separation step, containing unbound DNA fragments, was adjusted to 10 mM EDTA and 0.2% (w/v) SDS. Proteinase K and RNase A digestion were then performed as described above. After ethanol precipitation, DNA from the supernatant and from the bound fraction was dissolved in 50 μl H_2O.

Detection of Z-DNA fragments by PCR

A number of DNA primers were designed using the MacMolly® Tetra program package and synthesized as listed below. The digits in primer names indicate the length of the respective PCR products; primers correspond to either the upper strand (U) or lower strand (L). The numbers corresponding to the 5′ start nucleotides are shown in brackets for the c-*myc* *Hin*dIII–*Eco*RI fragment sequence published by Gazin *et al.* (1984) and stored at EMBL Nucleotide Sequence Database (Accession no. X00364). Lower case letters indicate additional nucleotides not belonging to the c-*myc* sequence that were added to yield longer PCR products.

Primer name: sequence
256U (605): CGGGTAATAACCCATCTTTGA
256L (861): GCCCAGCCCCACACAT
86U (904): TGCGGGTTACATACA
86L (989): GGCTGCCTTCCAGGCA
87U (1539): GCCCCACGGAAGCCTGA
87L (1626): CCTTCCACCCAGACTGA
301U (1675): CCCCCAACAAATGCAA
301L (1976): GCCCTCCACACAGAGA
218U (1985): CGCCTGCGATGATTTA
218L (2202): GGGGAGGGTGGGGAA
200U (3499): CCTGGGTCTCTAGAGGTGTTA
200L (3699): CCCGCTCCTCGCAGT
122U (3746): GGGGGAGGTATCGCA
122L (3867): CCGCGGGCTTTAACA
462U (3917): GGAGTGTTGGACGGGGGCGG
462L (4378): GGCTGGGTGGTCTTGGTGGGGG
85U (4401): GGGGAGAGGTTCGGGA
85L (4486): GCGGGAGGCAGTCTTGA
64U (4651): ccttggaaCGCCCAGCGAGGA
64L (4682): ccttggaaccttggaaccttggaaCTCGAATTTCTTCCAGATA
239U (5486): CCCGTTTGTCTCCCA
239L (5724): GCCCCTCATTTTTGTA
100U (5884): CCGCCCTCTTGGA
100L (5983): CTGAAATTGCTTGGTATGA
77U (6061): ccttggaaGGGTGTGTCCAAAGCCTCA
77L (6121): ccttggaaCCCAGGATAGGACATTGA

PCR was carried out in 50 μl of 1.5 mM $MgCl_2$, 0.1% (v/v) Triton X-100, 70 mM Tris−HCl, pH 8.8 containing 1 μl of DNA template solution and 30 pmol of each primer. After 5 min denaturation at 96°C, samples were kept at 90°C and 1 μl of dNTPs (10 mM) and 2.5 U Taq DNA polymerase (Ampli-Taq, Perkin-Elmer) were added to the hot sample. 20 cycles of amplification were carried out: 94°C for 1 min and 57°C for 1 min, then 2.5 U Taq DNA polymerase were added for another 15 cycles. PCR products were analyzed by gel electrophoresis on a 2% agarose gel with subsequent ethidium bromide staining. From the intensity of the bands, the yield of PCR products was estimated. For the gels shown in this paper, roughly equal quantities of DNA end products were loaded.

Detection of Z-DNA-containing fragments by hybridization

DNA fragments were separated on 8% polyacrylamide gels [acrylamide:bisacrylamide 29:1, 7 M urea, 1×Tris-borate-EDTA buffer (TBE)] of size 310×385×0.8 mm (BRL). After gel electophoreses, DNA was transferred to nylon membranes by electroblotting (Wölfl *et al.*, 1991). For this the gel was placed directly on a dry sponge-like material from air conditioner filters (Bartel, Berlin). The prewetted GeneScreen™ membrane was placed on top of the gel and the sandwich was topped with another dry sponge. It was slowly submerged in buffer avoiding air bubbles. Transfer was carried out in 0.5×TBE using 2.5 A (electrode separation 10 cm) in the cold for 40 min. Following transfer, DNA was immediately bound to the membrane by UV irradiation (254 nm) and subsequent heat treatment (80°C, 10 min). The conditions of UV irradiation are of importance for the generation of hybridization signals. Optimal conditions have to be established for each batch of nylon membrane.

Probes used for hybridization were generated by *in vitro* transcription from the following plasmid constructs. The 2.4 kb *Hin*dIII−*Xho*I fragment of the c-*myc* gene (5′ end) was inserted into the pGEM 4 Z vector (Promega). For probe synthesis, the plasmid was cut with *Eco*RI (at the *Xho*I end of the insert) and a 'sense' RNA probe was obtained by *in vitro* transcription using T7 RNA polymerase (Boehringer). A 2 kb *Pvu*II−*Eco*RI fragment of the c-*myc* gene (exon 3) was inserted into pBluescript II SK+ vector (Stratagene). For a 'sense' RNA probe, the plasmid was cut with *Bam*HI and transcribed with T7 RNA polymerase. The 'antisense' RNA probe covering exon 2 was transcribed with SP6 RNA polymerase from Amprobe™ human c-*myc* (Amersham). The 'antisense' RNA probe covering exon 1 was transcribed with T7 RNA polymerase from NENprobe™ human c-*myc* (NEN/DuPont). Synthesis was carried out with 250 μCi of [α-^{32}P]UTP (3000 Ci/mmol; NEN/DuPont).

Hybridization was carried out in an SDS−phosphate hybridization buffer [7% (w/v) SDS, 0.5 M NaH_2PO_4 pH 7.2, 1 mM EDTA, 1% (w/v) BSA] in rotating cylinders (Bachofer, Reutlingen, Germany) at 70°C. After 20 min of prehybridization in 30 ml hybridization buffer, membranes were hybridized in 5 ml hybridization buffer containing the specific radioactive probe. Only probes with $>5\times10^7$ c.p.m. were used.

After 16 h the nylon membranes were washed twice in wash buffer (WB) I [5% (w/v) SDS, 1 mM EDTA, 0.5% (w/v) BSA, 40 mM NaH_2PO_4, pH 7.2] at 60°C for 5 min and six times with WB II [1% (w/v) SDS, 1 mM EDTA, 40 mM NaH_2PO_4, pH 7.2] at 60°C for 5 min and once in WB III (100 mM NaH_2PO_4) at 70°C for 10 min. Membranes were dried on filter paper and autoradiography exposures were for 10−14 days.

Acknowledgements

This research was supported by grants to B.W. from the 'Fonds der Chemischen Industrie in Kooperation mit dem Bundesministerium für Forschung und Technologie (BMFT)' as well as the Trude Goerke Stiftung für Krebsforschung. A.R. was supported by grants from the National Institutes of Health, National Science Foundation, the Office of Naval Research and the American Cancer Society. We thank Dr Dirk Eick for the plasmid containing the c-*myc* gene and Anke-Schaubitzer-Meyer for expert technical assistance.

References

Beyer,A.L. and Osheim,Y.N. (1988) *Genes Dev.*, **2**, 754−765.
Budowsky,E.I. and Abdurashidova,G.G. (1989) *Prog. Nucleic Acids Res. Mol. Biol.*, **37**, 1−65.
Cole,M.D. (1986) *Annu. Rev. Genet.*, **20**, 361−384.
Dodd,R.C., Cohen,M.S., Newman,S.L. and Gray,T.K. (1983) *Proc. Natl Acad. Sci. USA*, **80**, 7538−7541.
Dorbic,T. and Wittig,B. (1987) *EMBO J.*, **6**, 2393−2399.
Dröge,P. and Nordheim,A. (1991) *Nucleic Acids Res.*, **19**, 2941−2946.
Eick,D. (1990) *Nucleic Acids Res.*, **18**, 1199−1205.
Eick,D. and Bornkamm,G.W. (1989) *EMBO J.*, **8**, 1965−1972.
Eick,D., Polack,A., Kofler,E., Lenoir,M.G., Rickinson,B.A. and Bornkamm,W.G. (1990) *Oncogene*, **5**, 1397−1402.
Einat,M., Resnitzky,D. and Kimchi,A. (1985) *Nature*, **313**, 597−600.
Ellison,M.J., Feigon,J., Kelleher,R.J., Wang,A.H.J., Habener,J.F. and Rich,A. (1986) *Biochemistry*, **25**, 3648−3655.
Gazin,C., Dupont de Dinechin,S., Hampe,A., Masson,J.-M., Martin,P., Stehelin,D. and Galibert,F. (1984) *EMBO J.*, **3**, 383−387.
Gidlund,M., Örn,A., Pattengale,P.K., Jansson,M., Wigzell,H. and Nilsson,K. (1981) *Nature*, **292**, 848−850.
Hill,J.R. (1991) *J. Cell Sci.*, **99**, 675−680.
Ho,P.S., Ellison,M.J., Quigley,G.J. and Rich,A. (1986) *EMBO J.*, **5**, 2737−2744.
Jackson,D.A. and Cook,P.R. (1985) *EMBO J.*, **4**, 913−918.
Jackson,D.A., Yuan,J. and Cook,P.R. (1988) *J. Cell Sci.*, **90**, 365−378.
Jimenez-Ruiz,A., Requena,J.M., Lopez,M.C. and Alonso,C. (1991) *Proc. Natl Acad. Sci. USA*, **88**, 31−35.
Johnston,H.B., Quigley,J.G., Ellison,J.M. and Rich,A. (1991) *Biochemistry*, **30**, 5257−5263.
Jovin,T.M., Soumpasis,D.M. and McIntosh,L.P. (1987) *Annu. Rev. Phys. Chem.*, **38**, 521−557.
Kagawa,T.F., Stoddard,D., Zhou,G. and Ho,P.S. (1989) *Biochemistry*, **28**, 6642−6651.
Karmali,R., Bhalla,A.K., Farrow,S.M., Williams,M.M., Lal,S., Lydyard,P.M. and O'Riordan,J.L.H. (1989) *J. Mol. Endocrinol.*, **3**, 43−48.
Kovalsky,O.I., Panyutin,I.G. and Budowsky,E.I. (1990) *Photochem. Photobiol.*, **52**, 509−517.
Lüscher,B. and Eisenman,R.N. (1990) *Genes Dev.*, **4**, 2025−2035.
Lafer,E.M., Möller,A., Nordheim,A., Stollar,B.D. and Rich,A. (1981) *Proc. Natl Acad. Sci. USA*, **78**, 3546−3550.
Larsson,L.-G., Ivhed,I., Gidlund,M., Pettersson,U., Vennström,B. and Nilsson,K. (1988) *Proc. Natl Acad. Sci. USA*, **85**, 2638−2642.
Liu,L.F. and Wang,J.C. (1987) *Proc. Natl Acad. Sci. USA*, **84**, 7024−7027.
Pauza,C.D., Galindo,J. and Richman,D.D. (1988) *J. Virol.*, **62**, 3558−3564.
Peck,L.J. and Wang,J.C. (1985) *Cell*, **40**, 129−137.
Piechaczyk,M., Yang,J.-Q., Blanchard,J.-M., Jeanteur,P. and Marcu,K.B. (1985) *Cell*, **42**, 589−597.
Piechaczyk,M., Blanchard,J.-M. and Jeanteur,P. (1987) *Trends Genet.*, **3**, 47−51.
Rahmouni,A.R. and Wells,R.D. (1989) *Science*, **246**, 358−363.
Rich,A., Nordheim,A. and Wang,A.H.J. (1984) *Annu. Rev. Biochem.*, **53**, 791−846.
Saiki,R.K., Gelfand,D.H., Stoffel,S., Scharf,S.J., Higuchi,R., Horn,G.T., Mullis,K.B. and Erlich,H.A. (1988) *Science*, **239**, 487−491.
Schroth,G.P., Chou,P.-J. and Ho,P.S. (1992) *J. Biol. Chem.*, **267**, 11846−11855.
Spencer,A.C. and Groudine,M. (1991) *Adv. Cancer Res.*, **56**, 1−48.
Stefanovsky,V.Y., Dimitrov,S.I., Russanova,V.R., Angelov,D. and Pashev,I.G. (1989) *Nucleic Acids Res.*, **17**, 10069−10081.
Stollar,B.D. (1986) *CRC Crit. Rev. Biochem.*, **20**, 1−36.
Sundström,C. and Nilsson,K. (1976) *Int. J. Cancer*, **17**, 565−577.
Vahrson,W. (1991) Thesis (Diplom Biochemie) at Freie Universität Berlin, Germany.
Wittig,B., Dorbic,T. and Rich,A. (1989) *J. Cell Biol.*, **108**, 755−764.
Wittig,B., Dorbic,T. and Rich,A. (1990) In Sarma,R.H. and Sarma,M.H. (eds), *Structure and Methods Volume 2: DNA Protein Complexes and Proteins*. Adenine Press, New York, pp. 1−23.
Wittig,B., Dorbic,T. and Rich,A. (1991) *Proc. Natl Acad. Sci. USA*, **88**, 2259−2263.
Wölfl,S., Schräder,M. and Wittig,B. (1991) *Proc. Natl Acad. Sci. USA*, **88**, 271−275.

Received on June 25, 1992; revised on August 18, 1992